NANO LETTERS

Letter

pubs.acs.org/NanoLett

Quasi-Ohmic Single Molecule Charge Transport through Highly Conjugated *meso*-to-*meso* Ethyne-Bridged Porphyrin Wires

Zhihai Li,[†,∥] Tae-Hong Park,[‡,∥,⊥] Jeff Rawson,[§] Michael J. Therien,*[,§] and Eric Borguet*[,†]

[†]Department of Chemistry, Temple University, Philadelphia, Pennsylvania 19122, United States

[‡]Department of Chemistry, 231 South 34th Street, University of Pennsylvania, Philadelphia, Pennsylvania 19104, United States

[§]Department of Chemistry, French Family Science Center, 124 Science Drive, Duke University, Durham, North Carolina 27708, United States

Supporting Information

ABSTRACT: Understanding and controlling electron transport through functional molecules are of primary importance to the development of molecular scale devices. In this work, the single molecule resistances of *meso*-to-*meso* ethyne-bridged (porphinato)zinc(II) structures (**PZn$_n$** compounds), connected to gold electrodes via (4′-thiophenyl)ethynyl termini, are determined using scanning tunneling microscopy-based break junction methods. These experiments show that each α,ω-di[(4′-thiophenyl)ethynyl]-terminated **PZn$_n$** compound (**dithiol-PZn$_n$**) manifests a dual molecular conductance. In both the high and low conductance regimes, the measured resistance across these metal−**dithiol-PZn$_n$**−metal junctions increases in a near linear fashion with molecule length. These results signal that *meso*-to-*meso* ethyne-bridged porphyrin wires afford the lowest β value (β = 0.034 Å^{-1}) yet determined for thiol-terminated single molecules that manifest a quasi-ohmic resistance dependence across metal−**dithiol-PZn$_n$**−metal junctions.

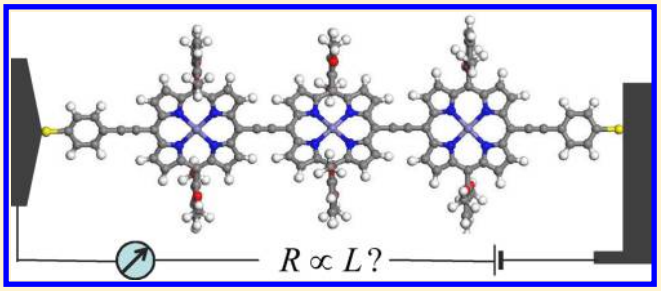

KEYWORDS: *Molecular conductance and devices, meso-to-meso ethyne-bridged (porphinato)zinc(II) wires, ohmic electron transport, STM break junction*

Controlling electron transport through molecular bridges that link two electrodes represents a basic step toward the development of sophisticated nanoscale devices.[1,2] As such, there is keen interest in the electrical properties of individual molecules and in understanding how parameters that include the nature of π-conjugation, magnitude of optical and potentiometric band gaps, molecular length, electrode material, and mode of molecule-to-electrode connectivity, impact molecular electrical conductance and transport mechanisms.[3−5]

A variety of techniques has been developed to construct metal−molecule−metal junctions and evaluate electrical functionality; these have included conducting atomic force microscopy,[6,7] crossed-wire tunnel junctions,[8] magnetic-bead junctions,[9] and nanopores[10,11] as well as mechanically controlled[12−14] and scanning probe microscopy (SPM) break junctions, i.e., scanning tunneling microscopy (STM) and conducting probe atomic force microscopy (C-AFM) break junctions.[2,15−22] These methods have been utilized to evaluate the conductances of widely varying molecular structures,[16,17,23] with SPM-based break junction techniques showing particular efficacy to interrogate conjugated structures having substantial length (>20 Å),[24−29] including oligophenyleneimines (OPIs),[7] butadiyne-bridged multi(porphyrin) systems,[15,28] oligothiophenes,[24] poly(*p*-phenyleneethynylene)s,[25] oligo(pentaphenylene)s,[26] and oligo(tetrathiafulvalene-pyromellitic-diimide-imine)s.[27] Frisbie et al. have chronicled a change in charge transport mechanism in OPIs from tunneling to hopping as a function of molecular wire length,[7] while Tao et al. have detected a similar mechanistic transition through temperature-dependent measurements of conductance.[26] Nichols, Anderson, and co-workers have reported recently analyses of temperature-dependent conductance measurements that suggest that phase coherent tunneling, as opposed to charge hopping, is responsible for the weak length dependence of the measured conductance in butadiyne-bridged multi(porphyrin)-based wires.[15,28]

Charge transport through metal−molecule−metal (m−M−m) junctions has been investigated by measuring conductance (or resistance) as a function of molecular length (L).[15,17] In the tunneling regime, where most molecular junctions operate,[17,28] the junction resistance (R) increases approximately exponentially with L, and correspondingly the magnitudes of measured molecular conductances (σ_M values) decrease exponentially with molecular length. The junction resistance is described by eq 1:

$$R = R_0 \exp(\beta L) \tag{1}$$

Received: December 7, 2011
Revised: March 30, 2012
Published: April 12, 2012

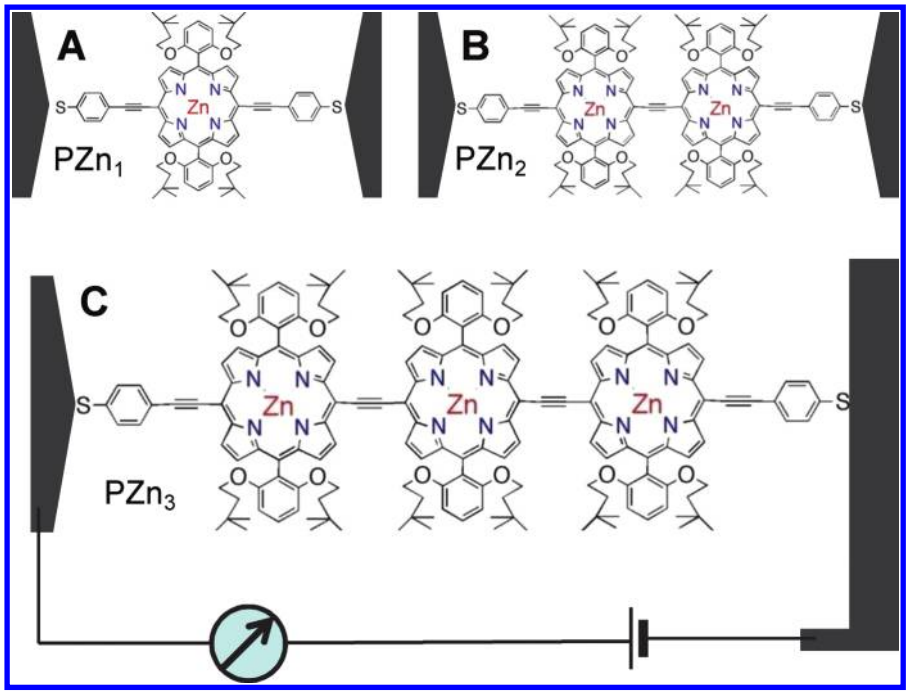

Figure 1. Schematic describing STM break junction-based single molecule conductance measurements for the α,ω-di[(4′-thiophenyl)ethynyl]-terminated $\mathbf{PZn}_n$ compounds (**dithiol-PZn$_1$** (A), **dithiol-PZn$_2$** (B), and **dithiol-PZn$_3$** (C)) examined in this study.

Here R_0 is an effective contact resistance and β is a decay constant for transmission across a barrier extracted from fitting an exponential to experimental resistance values; β depends on the structure of the molecular backbone and characterizes the distance dependence of the experimentally determined single molecule resistance. For the typical case, where the metal Fermi energies are off resonance with the molecular cation or anion state energies, molecule-mediated tunneling (superexchange) governs transport in m−M−m junctions; the resistance across such junctions gives rise to an approximate exponential decay of measured conductance with increasing molecular length. While single-step tunneling is mediated by the eigenstates of the bridging molecule, these states are populated only virtually, and the tunneling rate decays exponentially with molecular length. On the other hand, when metal Fermi energies are resonant with the relevant bridge states, electrons (or holes) are injected directly into the bridging molecule; in such cases, the distance dependence of the conductance is weak, and correspondingly small values of β, consistent with transport via carrier injection, are manifest.[17] Relatively few molecular wire systems have been delineated that display near-linear dependences of conductance with molecular length (i.e., $\beta < 0.1$ Å^{-1}).[15,17,25] While both molecular wire topology and the nature of molecule-to-electrode connectivity[17] play important roles in modulating charge transport barriers and mechanisms, it is an open question whether molecular design can provide organic single molecules that manifest ohmic behavior ($R \propto L$).

Relative to many classes of conjugated structures for which single molecule charge transport measurements have been made, *meso*-to-*meso* ethyne-bridged (porphinato)zinc(II) structures ($\mathbf{PZn}_n$ compounds, Figure 1) manifest exceptional electronic structural characteristics. These include: (i) low-energy $\pi-\pi^*$ excited states that are polarized exclusively along the long molecular axis; (ii) intensely absorbing $S_1 \rightarrow S_n$ transitions that extend deep into the near-infrared spectral region; (iii) the largest hole polaron delocalization lengths yet measured for single molecules; (iv) impressive dark and photo conductivities; and (v) unusually large polarizabilities.[30−45] Congruently, these structures have been utilized in a number of nanoscale devices that take advantage of their remarkable optoelectronic properties.[46,47]

In this work, $\mathbf{PZn}_n$ single molecule conductances are investigated using STM break junction methods. In order to facilitate comparisons to the significant body of measured single molecule conductances determined across Au−molecule−Au junctions, we exploit thiol-based anchoring groups in these structures. Our results show that there are two sets of molecular conductance values for each α,ω-di[(4′-thiophenyl)ethynyl]-terminated $\mathbf{PZn}_n$ structure (**dithiol-PZn$_n$**, Figure 1) and that the measured resistances across metal−**dithiol-PZn$_n$**−metal junctions increase in a near linear fashion with molecule length. The β value determined experimentally from the length dependence of **dithiol-PZn$_n$** resistance corresponds to 0.034 Å^{-1}; these structures thus afford the lowest β value yet determined for thiol-terminated single molecules.

The design, synthesis, and characterization of *S*-acetyl-protected α,ω-di[(4′-thiophenyl)ethynyl]-terminated $\mathbf{PZn}_n$ compounds ($\mathbf{PZn}_n$**-SAc** structures) as well as details concerning the STM break junction experiments are described in the Supporting Information. Individual current−distance traces obtained for **dithiol-PZn$_1$** (Figure 2A) were determined utilizing a sample prepared by a short time (2 min) assembly procedure (Supporting Information) and measured at a tip−sample separation rate of 10 nm·s^{-1}. In these experiments, note that the current first decreased exponentially as the tip−substrate separation increased and then plateaued, before the current dropped down close to zero (Figure 2A). The current steps/plateaus chronicle the bias voltage-dependent conductances[2] of molecular junctions formed between the two electrodes.

Three types of current−distance traces were observed in these experiments: (i) those having low-conductance (LC)

dx.doi.org/10.1021/nl2043216 | *Nano Lett.* 2012, 12, 2722−2727

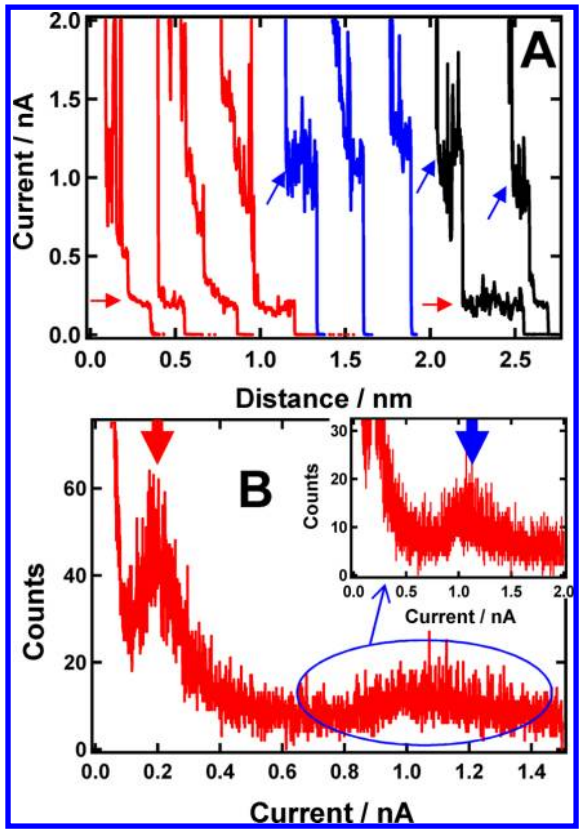

Figure 2. (A) Exemplary current−distance traces recorded during STM break junction experiments for **dithiol-PZn$_1$** molecular junctions at V_{bias} = 0.10 V. Red, blue, and black responses represent typical respective low, high, and mixed LC/HC traces. (B) Histogram analysis of **dithiol-PZn$_1$** conductance determined from STM break junction experiments carried out at V_{bias} = 0.10 V. Arrows indicate low- and high-current (red and blue, respectively) steps (A) and LC and HC current peaks (B). The inset shows the magnification of the peak in the HC region of (B).

Table 1. Molecular Lengths, Single Molecule Conductances, and Molecular Resistances of dithiol-PZn$_{1-3}$ Structures

molecule	**dithiol-PZn$_1$**	**dithiol-PZn$_2$**	**dithiol-PZn$_3$**
length (Å)[a]	24.3	35.2	46.1
conductance (nS)	2.21 ± 0.31 (LC)	1.56 ± 0.12 (LC)	1.05 ± 0.10 (LC)
	9.91 ± 1.02 (HC)	6.99 ± 0.49 (HC)	4.67 ± 0.78 (HC)
resistance (GΩ)	0.45 ± 0.06 (LC)	0.64 ± 0.05 (LC)	0.95 ± 0.11 (LC)
	0.10 ± 0.01 (HC)	0.14 ± 0.01 (HC)	0.21 ± 0.03 (HC)

[a]Corresponds to the S atom-to-S atom distance for α,ω-di[(4′-thiophenyl)ethynyl]-terminated **PZn$_n$** compounds computed from molecular geometry optimization (Accelrys Materials Studio).

current steps (red traces, Figure 2A); (ii) those having high-conductance (HC) current steps (blue traces, Figure 2A); and (iii) those that feature both types of conductance steps (black traces, Figure 2A). Note that HC steps are noisier than LC steps (Figure 2A) and result in a broader current peak in the Figure 2B current histogram. While the ratio of observed LC:HC current−distance traces is ∼2:1, note that traces featuring both LC and HC values are infrequent (∼0.3% of all recorded traces for **dithiol-PZn$_1$** and ∼1% and 0.6% for **dithiol-PZn$_2$**- and **dithiol-PZn$_3$**-based molecular junctions, respectively. (See Figures S3 and S4, Supporting Information).

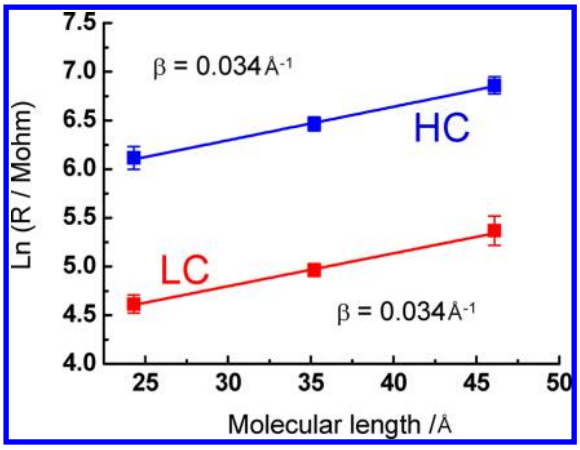

Figure 3. Natural logarithmic plots of measured resistance versus molecular length for **dithiol-PZn$_{1-3}$** structures. The red and blue lines correspond to separate analyses of the resistance values obtained respectively from the LC and HC data. The β values are calculated through the semilogarithmic plot of resistance and molecule length based on $R = R_0 \exp(\beta L)$.

The Figure 2B histogram analysis of **dithiol-PZn$_1$** conductance shows current maxima of 0.22 ± 0.03 and 0.99 ± 0.10 nA, corresponding to molecular conductances of 2.2 and 9.9 nS, respectively, at the V_{bias} of 0.10 V (Table 1). Experiments at other bias voltages (0.05, 0.10, 0.20 V) provide a current vs V_{bias} plot and yield consistent values of 2.23 ± 0.26 nS (2.88×10^{-5} G_o) and 9.91 ± 1.15 nS (1.28×10^{-4} G_o) for the respective LC and HC. No difference was observed between the positive bias and negative bias [i.e., bias voltages of 0.1 and −0.1 give identical molecular conductance values for these **dithiol-PZn$_n$** systems (Figure S2, Supporting Information)]. Note that the **dithiol-PZn$_1$** LC value is comparable to that reported for a related functionalized (porphinato)zinc(II) monomer (2.13 ± 0.28 nS; 2.75×10^{-5} G_o) investigated by Anderson, Nichols et al.[15] However, these investigators did not observe a corresponding HC response similar to that described.

While measured dual conductances have not been reported previously for porphyrin-based single molecules, dual/multiple conductances have been reported in other molecular systems interrogated via STM break junction methods.[48−52] Multiple conductance responses are generally thought to derive from variations in the molecule−electrode contact geometry or changes in molecular conformation or geometry in the junction that occur during stretching within the STM gap.[53] For instance, Wandlowski et al.[50] ascribed the origin of three measured conductance values to three possible molecular conformations, while Haiss et al.[54] attributed three measured conductance values to differences in the contact geometry between the electrodes and the molecular thiol termini. Tao et al. noted dual conductances for octanedithiols in Au−molecule−Au junctions and interpreted these results as arising from possible molecule−electrode contact geometries in which the thiol group is positioned on either a gold pyramidal (top) or a gold pyramidal vacancy (hollow) site.[48] According to the hypothesis put forth by Tao and co-workers, thiol connectivity to a hollow site provides a larger conductance than binding to a top site.[48] These authors report an observed HC:LC ratio of 2:1, consistent with the top:hollow site ratio.[48] As the **dithiol-PZn$_n$** conductance data feature an HC:LC ratio of ∼1:2, the observed dual conductance behavior may not trace its genesis to the effect described by Tao et al., unless the potential energy

dx.doi.org/10.1021/nl2043216 | Nano Lett. 2012, 12, 2722−2727

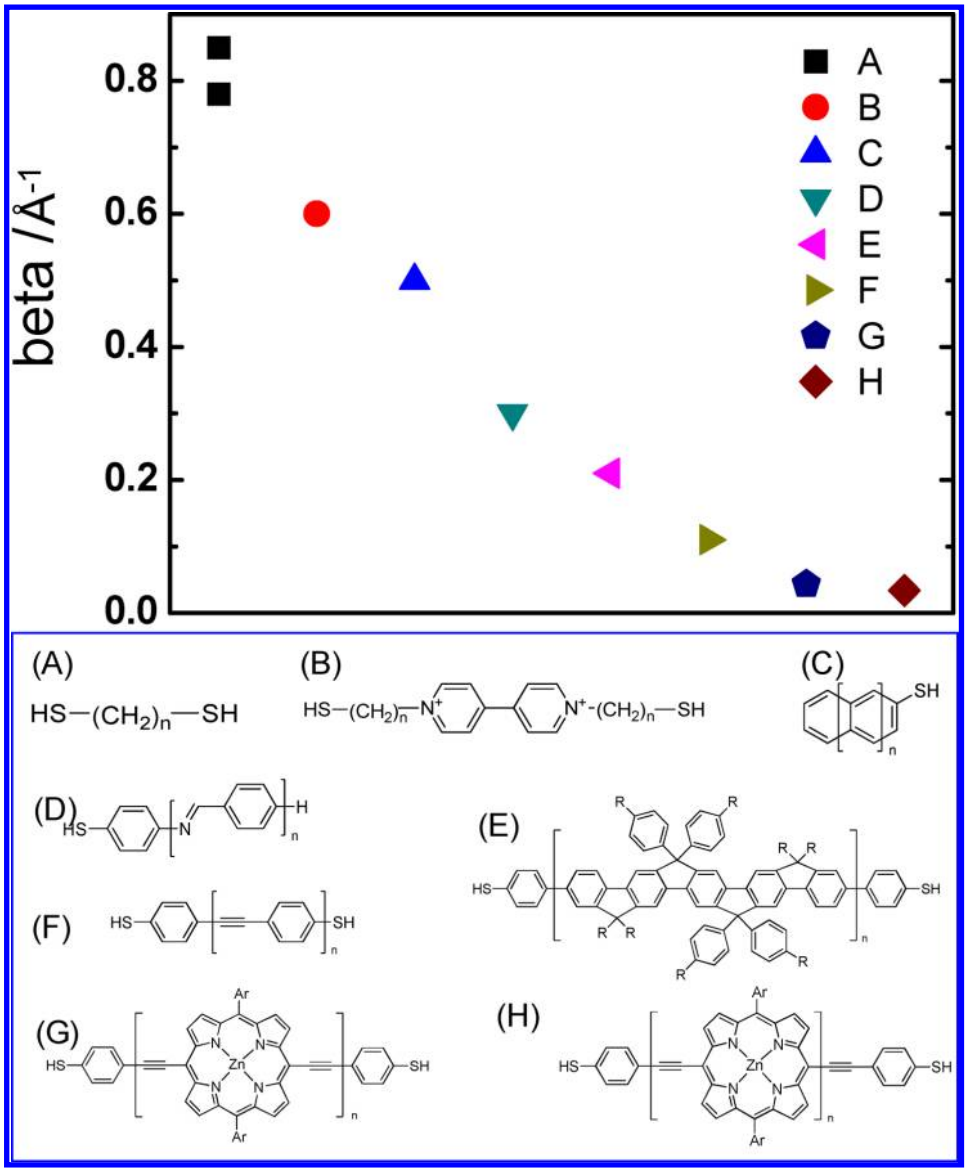

Figure 4. Comparative distance dependences of experimentally evaluated single molecule resistances determined from charge transport measurements across Au−molecule−Au junctions for benchmark thiol-terminated molecular wire frameworks. For these systems, β was determined from an analysis of distance-dependent molecular resistance data based on eq 1 [$R = R_0 \exp(\beta L)$]: (A) alkanes;[23,50] (B) alkane-viologen hybrids;[18] (C) oligoacenes;[55] (D) oligophenyleneimines;[7] (E) oligo(*p*-fluorene)s;[29] (F) oligo(*p*-phenyleneethynylene)s;[17,25] (G) *meso*-to-*meso* butadiyne-bridged (porphinato)zinc oligomers;[15] and (H) *meso*-to-*meso* ethyne-bridged (porphinato)zinc wires (**dithiol-PZn$_n$** structures; this work).

surfaces for Au top and hollow sites are significantly modified by **dithiol-PZn$_n$** attachment relative to those which exist for octanedithiol.

While ascribing origins to the multiple conductance responses of molecules can be controversial, the rigid, conformationally inflexible nature of **dithiol-PZn$_n$** structures suggest that the observed dual conductance in the present study is not a consequence of different possible molecular conformations but is likely congruent with a model proposed recently by Venkataraman et al.,[49] in which LC values derive from charge transport through fully stretched molecules within the junction, while HC stems from transport through molecules bound at an angle with respect to the electrode surface normal.

Similarly for **dithiol-PZn$_2$** and **dithiol-PZn$_3$**, 10 000−20 000 current−distance traces were recorded for a given bias voltage, and identical statistical analyses were utilized to determine single molecule resistance and conductance values. Typical STM images of molecule-modified electrode surfaces, exemplary current−distance traces, and corresponding conductance histogram analyses for **dithiol-PZn$_2$** and **dithiol-PZn$_3$** can be found in Figures S3 and S4, Supporting Information. Akin to **dithiol-PZn$_1$**, dual conductances were also detected for both **dithiol-PZn$_2$** and **dithiol-PZn$_3$**. Interestingly, these data demonstrate that the measured resistances of these *meso*-to-*meso* ethyne-bridged (porphinato)zinc(II) structures increase only marginally with increasing m−M−m distance; note that for **dithiol-PZn$_{1-3}$**, R increases from 0.45 ± 0.06 to 0.95 ± 0.11 GΩ in the LC regime and from 0.10 ± 0.01 to 0.21 ± 0.03 GΩ in the HC regime, as molecular length increases from 24.3 to 46.1 Å (Table 1). The near-linear relationship of resistance vs molecular length (Figure 3) suggests quasi-ohmic charge transport characteristics for **dithiol-PZn$_n$** wires. Note that the β values determined from the length dependence of the measured **dithiol-PZn$_n$** resistances correspond to 0.034 ±

dx.doi.org/10.1021/nl2043216 | *Nano Lett.* 2012, 12, 2722−2727

0.007 and 0.034 ± 0.006 Å^{-1}, respectively, for the LC and HC data. Placing these results within the broader context of benchmark molecular wire frameworks that utilize thiol-based anchoring groups for which the distance dependence of single molecule resistance has been determined from charge transport measurements across Au−molecule−Au junctions (Figure 4), the β values for **dithiol-PZn$_n$** wires represent the smallest yet determined for thiol-terminated single molecules. It is also noteworthy that the β values determined for **dithiol-PZn$_n$** are diminished relative to that reported by Anderson, Nichols et al. for corresponding *meso*-to-*meso* butadiyne-bridged (porphinato)zinc oligomers (0.04 ± 0.006 Å^{-1}).[15,28] Given the Anderson−Nichols temperature-dependent transport data congruent with a coherent charge transport mechanism[28] and the established relationship of the potentiometrically determined frontier orbital energies of ethyne- and butadiyne-bridged (porphinato)zinc structures,[35,38] we posit that these **dithiol-PZn$_n$** wires similarly manifest apparent coherent charge transport.

In conclusion, single molecule resistances of *meso*-to-*meso* ethyne-bridged (porphinato)zinc(II) structures (**PZn$_n$** compounds) interconnected to gold electrodes via (4′-thiophenyl)-ethynyl termini were determined using STM break junction methods. These experiments show that each α,ω-di[(4′-thiophenyl)ethynyl]-terminated **PZn$_n$** compound (**dithiol-PZn$_n$**) manifests a dual molecular conductance; congruent with earlier literature, the LC values derive likely from charge transport through a fully stretched molecule within the junction, while the measured HC stems from transport through a molecule bound at an angle with respect to the electrode surface normal. In both the HC and LC regimes, the measured resistance across these metal−**dithiol-PZn$_n$**−metal junctions increases in a near linear fashion with molecule length. The decay constants β, extracted from fitting an exponential to these distance-dependent experimental resistance values, are 0.034 ± 0.007 and 0.034 ± 0.006 Å^{-1}, respectively, for the LC and HC data. Due to the small magnitude of β determined for these **dithiol-PZn$_n$** structures, it is important to underscore that tunneling, resonant, and hopping processes may all contribute to current mediation. The combination of apparent coherent single molecule charge transport and β = 0.034 Å^{-1} gives rise to a quasi-ohmic resistance dependence across metal−**dithiol-PZn$_n$**−metal junctions. This work motivates further studies that (i) probe the extent to which tunneling and resonant transport mechanisms operate in these systems and (ii) examine the degree to which m−M−m junction resistances may be diminished through modulation of molecule−electrode electronic coupling.[17]

■ ASSOCIATED CONTENT

Supporting Information

Detailed experimental and synthetic procedures, characterization data; individual current−distance traces and single molecule conductance histograms for **dithiol-PZn$_2$** and **dithiol-PZn$_3$**; and STM images of molecule-modified electrode surface. This material is available free of charge via the Internet at http://pubs.acs.org.

■ AUTHOR INFORMATION

Corresponding Author

*E-mail: michael.therien@duke.edu; eborguet@temple.edu.

Present Address

[⊥]Nuclear Chemistry Research Division, Korea Atomic Energy Research Institute (KAERI), Daejeon, 305−353, Korea

Author Contributions

[∥]These authors contributed equally.

Notes

The authors declare no competing financial interest.

■ ACKNOWLEDGMENTS

The authors are grateful to Dr. Yangjun Xing for his assistance with the software for statistical analysis of single molecule conductance data. E.B. thanks the National Science Foundation (CHE 0809838) for financial support, and support of Z.L. M.J.T. is grateful to the National Science Foundation (NSEC DMR04-25780) for infrastructural support, and support of T.H.P.; M.J.T. is grateful to the UNC EFRC: Center for Solar Fuels, an Energy Frontier Research Center funded by the U.S. Department of Energy, Office of Science, Office of Basic Energy Sciences under Award Number DE-SC0001011, for its support of J.R.

■ REFERENCES

(1) Nitzan, A.; Ratner, M. A. *Science* **2003**, *300*, 1384−1389.
(2) Xu, B. Q.; Tao, N. J. *Science* **2003**, *301*, 1221−1223.
(3) McCreery, R. L.; Bergren, A. J. *Adv. Mater.* **2009**, *21*, 4303−4322.
(4) van der Molen, S. J.; Liljeroth, P. *J. Phys.: Condens. Matter* **2010**, *22*, 133001−133030.
(5) Scullion, L.; Doneux, T.; Bouffier, L.; Fernig, D. G.; Higgins, S. J.; Bethell, D.; Nichols, R. J. *J. Phys. Chem. C* **2011**, *115*, 8361−8368.
(6) Morita, T.; Lindsay, S. *J. Am. Chem. Soc.* **2007**, *129*, 7262−7263.
(7) Choi, S. H.; Kim, B.; Frisbie, C. D. *Science* **2008**, *320*, 1482−1486.
(8) Kushmerick, J. G.; Holt, D. B.; Pollack, S. K.; Ratner, M. A.; Yang, J. C.; Schull, T. L.; Naciri, J.; Moore, M. H.; Shashidhar, R. *J. Am. Chem. Soc.* **2002**, *124*, 10654−10655.
(9) Blum, A. S.; Kushmerick, J. G.; Long, D. P.; Patterson, C. H.; Yang, J. C.; Henderson, J. C.; Yao, Y. X.; Tour, J. M.; Shashidhar, R.; Ratna, B. R. *Nat. Mater.* **2005**, *4*, 167−172.
(10) Lee, T.; Wang, W. Y.; Klemic, J. F.; Zhang, J. J.; Su, J.; Reed, M. A. *J. Phys. Chem. B* **2004**, *108*, 8742−8750.
(11) Tsutsui, M.; Taniguchi, M.; Yokota, K.; Kawai, T. *Nat. Nanotechnol.* **2010**, *5*, 286−290.
(12) Reed, M. A.; Zhou, C.; Muller, C. J.; Burgin, T. P.; Tour, J. M. *Science* **1997**, *278*, 252−254.
(13) Gonzalez, M. T.; Wu, S. M.; Huber, R.; van der Molen, S. J.; Schonenberger, C.; Calame, M. *Nano Lett.* **2006**, *6*, 2238−2242.
(14) Reichert, J.; Ochs, R.; Beckmann, D.; Weber, H. B.; Mayor, M.; von Lohneysen, H. *Phys. Rev. Lett.* **2002**, *88*, 176804.
(15) Sedghi, G.; Sawada, K.; Esdaile, L. J.; Hoffmann, M.; Anderson, H. L.; Bethell, D.; Haiss, W.; Higgins, S. J.; Nichols, R. J. *J. Am. Chem. Soc.* **2008**, *130*, 8582−8583.
(16) Venkataraman, L.; Klare, J. E.; Nuckolls, C.; Hybertsen, M. S.; Steigerwald, M. L. *Nature* **2006**, *442*, 904−907.
(17) Xing, Y. J.; Park, T.-H.; Venkatramani, R.; Keinan, S.; Beratan, D. N.; Therien, M. J.; Borguet, E. *J. Am. Chem. Soc.* **2010**, *132*, 7946−7956.
(18) Li, Z. H.; Pobelov, I.; Han, B.; Wandlowski, T.; Blaszczyk, A.; Mayor, M. *Nanotechnology* **2007**, *18*, 044018.
(19) Kiguchi, M.; Takahashi, T.; Kanehara, M.; Teranishi, T.; Murakoshi, K. *J. Phys. Chem. C* **2009**, *113*, 9014−9017.
(20) Qian, G. G.; Saha, S.; Lewis, K. M. *Appl. Phys. Lett.* **2010**, *96*, 243107.
(21) Zhou, X. S.; Liu, L.; Fortgang, P.; Lefevre, A. S.; Serra-Muns, A.; Raouafi, N.; Amatore, C.; Mao, B. W.; Maisonhaute, E.; Schollhorn, B. *J. Am. Chem. Soc.* **2011**, *133*, 7509−7516.

(22) Li, Z.; Han, B.; Meszaros, G.; Pobelov, I.; Wandlowski, T.; Blaszczyk, A.; Mayor, M. *Faraday Discuss.* **2006**, *131*, 121−143.
(23) Chen, F.; Li, X. L.; Hihath, J.; Huang, Z. F.; Tao, N. J. *J. Am. Chem. Soc.* **2006**, *128*, 15874−15881.
(24) Yamada, R.; Kumazawa, H.; Tanaka, S.; Tada, H. *Appl. Phys. Express* **2009**, *2*, 025002(1−3).
(25) Lu, Q.; Liu, K.; Zhang, H. M.; Du, Z. B.; Wang, X. H.; Wang, F. S. *ACS Nano* **2009**, *3*, 3861−3868.
(26) Hines, T.; Diez-Perez, I.; Hihath, J.; Liu, H. M.; Wang, Z. S.; Zhao, J. W.; Zhou, G.; Muellen, K.; Tao, N. J. *J. Am. Chem. Soc.* **2010**, *132*, 11658−11664.
(27) Choi, S. H.; Frisbie, C. D. *J. Am. Chem. Soc.* **2010**, *132*, 16191−16201.
(28) Sedghi, G.; García-Suárez, V. M.; Esdaile, L. J.; Anderson, H. L.; Lambert, C. J.; Martin, S.; Bethell, D.; Higgins, S. J.; Elliott, M.; Bennett, N.; Macdonald, J. E.; Nichols, R. J. *Nat. Nanotechnol.* **2011**, 517−522.
(29) Lafferentz, L.; Ample, F.; Yu, H.; Hecht, S.; Joachim, C.; Grill, L. *Science* **2009**, *323*, 1193−1197.
(30) Lin, V. S. Y.; DiMagno, S. G.; Therien, M. J. *Science* **1994**, *264*, 1105−1111.
(31) Lin, V. S. Y.; Therien, M. J. *Chem.−Eur. J.* **1995**, *1*, 645−651.
(32) Angiolillo, P. J.; Lin, V. S. Y.; Vanderkooi, J. M.; Therien, M. J. *J. Am. Chem. Soc.* **1995**, *117*, 12514−12527.
(33) Shediac, R.; Gray, M. H. B.; Uyeda, H. T.; Johnson, R. C.; Hupp, J. T.; Angiolillo, P. J.; Therien, M. J. *J. Am. Chem. Soc.* **2000**, *122*, 7017−7033.
(34) Rubtsov, I. V.; Susumu, K.; Rubtsov, G. I.; Therien, M. J. *J. Am. Chem. Soc.* **2003**, *125*, 2687−2696.
(35) Susumu, K.; Therien, M. J. *J. Am. Chem. Soc.* **2002**, *124*, 8550−8552.
(36) Fletcher, J. T.; Therien, M. J. *Inorg. Chem.* **2002**, *41*, 331−341.
(37) Ostrowski, J. C.; Susumu, K.; Robinson, M. R.; Therien, M. J.; Bazan, G. C. *Adv. Mater.* **2003**, *15*, 1296−1300.
(38) Susumu, K.; Duncan, T. V.; Therien, M. J. *J. Am. Chem. Soc.* **2005**, *127*, 5186−5195.
(39) Ghoroghchian, P. P.; Frail, P. R.; Susumu, K.; Blessington, D.; Brannan, A. K.; Bates, F. S.; Chance, B.; Hammer, D. A.; Therien, M. J. *Proc. Natl. Acad. Sci. U.S.A.* **2005**, *102*, 2922−2927.
(40) Susumu, K.; Frail, P. R.; Angiolillo, P. J.; Therien, M. J. *J. Am. Chem. Soc.* **2006**, *128*, 8380−8381.
(41) Duncan, T. V.; Susumu, K.; Sinks, L. E.; Therien, M. J. *J. Am. Chem. Soc.* **2006**, *128*, 9000−9001.
(42) Duncan, T. V.; Wu, S. P.; Therien, M. J. *J. Am. Chem. Soc.* **2006**, *128*, 10423−10435.
(43) Frail, P. R.; Susumu, K.; Huynh, M.; Fong, J.; Kikkawa, J. M.; Therien, M. J. *Chem. Mater.* **2007**, *19*, 6062−6064.
(44) Duncan, T. V.; Ishizuka, T.; Therien, M. J. *J. Am. Chem. Soc.* **2007**, *129*, 9691−9703.
(45) Fisher, J. A. N.; Susumu, K.; Therien, M. J.; Yodh, A. G. *J. Chem. Phys.* **2009**, *130*, 134506(1−8).
(46) Banerjee, P.; Conklin, D.; Nanayakkara, S.; Park, T. H.; Therien, M. J.; Bonnell, D. A. *ACS Nano* **2010**, *4*, 1019−1025.
(47) Conklin, D.; Park, T.-H.; Nanayakkara, D.; Therien, M. J.; Bonnell, D. A. *Adv. Funct. Mater.* **2011**, *21*, 4712−4718.
(48) Li, X. L.; He, J.; Hihath, J.; Xu, B. Q.; Lindsay, S. M.; Tao, N. J. *J. Am. Chem. Soc.* **2006**, *128*, 2135−2141.
(49) Kamenetska, M.; Quek, S. Y.; Whalley, A. C.; Steigerwald, M. L.; Choi, H. J.; Louie, S. G.; Nuckolls, C.; Hybertsen, M. S.; Neaton, J. B.; Venkataraman, L. *J. Am. Chem. Soc.* **2010**, *132*, 6817−6821.
(50) Li, C.; Pobelov, I.; Wandlowski, T.; Bagrets, A.; Arnold, A.; Evers, F. *J. Am. Chem. Soc.* **2008**, *130*, 318−326.
(51) Martin, S.; Haiss, W.; Higgins, S. J.; Nichols, R. J. *Nano Lett.* **2010**, *10*, 2019−2023.
(52) Zhou, X. S.; Chen, Z. B.; Liu, S. H.; Jin, S.; Liu, L.; Zhang, H. M.; Xie, Z. X.; Jiang, Y. B.; Mao, B. W. *J. Phys. Chem. C* **2008**, *112*, 3935−3940.
(53) Kim, Y.; Song, H.; Strigl, F.; Pernau, H. F.; Lee, T.; Scheer, E. *Phys. Rev. Lett.* **2011**, *106*, 196804(1−4).
(54) Haiss, W.; Martin, S.; Leary, E.; van Zalinge, H.; Higgins, S. J.; Bouffier, L.; Nichols, R. J. *J. Phys. Chem. C* **2009**, *113*, 5823−5833.
(55) Kim, B.; Beebe, J. M.; Jun, Y.; Zhu, X. Y.; Frisbie, C. D. *J. Am. Chem. Soc.* **2006**, *128*, 4970−4971.

NOTE ADDED AFTER ASAP PUBLICATION

This paper was published ASAP on May 4, 2012. The Acknowledgments and Reference 47 have been updated. The revised version was posted on May 14, 2012.